Available online at www.sciencedirect.com

ScienceDirect

Mendeleev Commun., 2024, **34**, 119–121

Mendeleev Communications

Myrtenyl-bispidine containing azole: synthesis and antifungal activity

Nikolai S. Li-Zhulanov,[a] Konstantin Yu. Ponomarev,[a] Suat Sari,[b] Dolunay Gülmez,[c] Sevtap Arikan-Akdagli,[c] Vyacheslav I. Krasnov,[a] Evgenii V. Suslov,[a] Konstantin P. Volcho*[a] and Nariman F. Salakhutdinov[a]

[a] *N. N. Vorozhtsov Novosibirsk Institute of Organic Chemistry, Siberian Branch of the Russian Academy of Sciences, 630090 Novosibirsk, Russian Federation. E-mail: volcho@nioch.nsc.ru*
[b] *Department of Pharmaceutical Chemistry, Hacettepe University Faculty of Pharmacy, Sihhiye, 06100 Ankara, Turkey*
[c] *Department of Medical Microbiology, Hacettepe University Faculty of Medicine, Sihhiye, 06100 Ankara, Turkey*

DOI: 10.1016/j.mencom.2024.01.036

A new monoterpene–azole hybrid containing myrtenyl-bispidine moiety, 2-(2,4-difluorophenyl)-1-(7-{[(1*R*,5*S*)-6,6-dimethylbicyclo[3.1.1]hept-2-en-2-yl]methyl}-1,5-dimethyl-3,7-diazabicyclo[3.3.1]non-3-yl)-3-(1*H*-1,2,4-triazol-1-yl)-propan-2-ol was prepared in six steps with 55% overall yield. The compound was tested against a number of *Candida spp*. fungi and found to be active against *Candida albicans*. Molecular docking suggested possible inhibition of lanosterol 14α-demethylase (CYP51), a membrane enzyme targeted by azole antifungals.

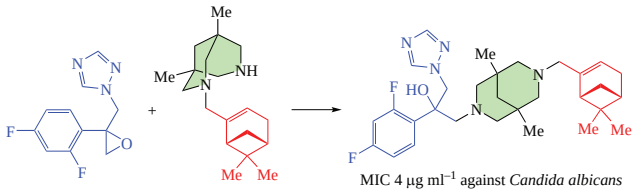

Keywords: azoles, hybrids, *Candida spp*., bispidine, monoterpenes, myrtenol.

Fungal infections pose a significant public health concern, as there are over 600 species of pathogenic fungi that can cause human diseases and there are no licensed vaccines to prevent them. In October 2022, the World Health Organization published a list of Fungal Priority Pathogens, highlighting the urgency for action.[1] Limited availability of the most effective drugs to treat fungal infections in regions where they are prevalent and the emergence of species that are resistant to current therapies exacerbate the problem. For a long time, azoles have been the primary antifungal class used to combat mycoses. However, the emergence of drug-resistant strains and the resulting rise in mortality rates of systemic mycoses have necessitated the development of new-generation, broad-spectrum azole antifungal agents.[2]

Earlier, several monoterpene-containing hybrid azoles were synthesized and found to show potent antifungal activity against both azole-susceptible and azole-resistant strains of *Candida spp*. In our latest study,[3] one of the compounds with myrtenyl fragment **1** (Figure 1) demonstrated up to 60 times lower minimum inhibitory concentration (MIC) values than fluconazole against clinical isolates. Activity of the monoterpenoid (−)-myrtenol against both yeast (*Candida albicans*) and mycelial (*Rhizopus nigricans*, *Aspergillus fumigatus*, *Fusarium solani*) fungi species was showed.[4] Akhmedov *et al*.[5] recently reported synthesis of a series of imidazole terpenoid derivatives with good activity against *Candida spp*. Sulfur-containing terpenoids of bornane and pinane series also showed moderate antifungal activity against several mold and yeast-like fungi.[6–8] Thus, in an attempt to obtain new and potent antifungal monoterpene–azole hybrids, herein, synthesis of a new analogue of compound **1** with bispidine linker instead of piperazine, *viz*. 2-(2,4-difluorophenyl)-1-(7-{[(1*R*,5*S*)-6,6-dimethylbicyclo[3.1.1]hept-2-en-2-yl]-methyl}-1,5-dimethyl-3,7-diazabicyclo[3.3.1]nonan-3-yl)-3-(1*H*-1,2,4-triazol-1-yl)propan-2-ol **2** (see Figure 1), its antifungal activity and molecular modeling studies are presented. The 3,7-diazabicyclo[3.3.1]nonane (bispidine) framework is considered as a part of the 'privileged structures' within medicinal chemistry due to the broad and varied range of biological activities observed in compounds containing this structural motif.[9,10]

Initially, epoxide **5** was prepared from 2-chloro-1-(2,4-difluorophenyl)ethan-1-one **3** (Scheme 1) according to the known method.[3] Alkylation of 1,2,4-triazole with chloride **3** gave ketone **4** in 80% yield. The carbonyl group of ketone **4** was subsequently transformed into epoxide *via* the Corey–Chaykovsky reaction using trimethylsulfoxonium iodide $Me_3S^+OI^-$, resulting in oxirane **5** with a yield of 90% (see Scheme 1).

For the synthesis of myrtenyl-bispidine building block **8**, we performed the reaction between diazaadamantane **6** and

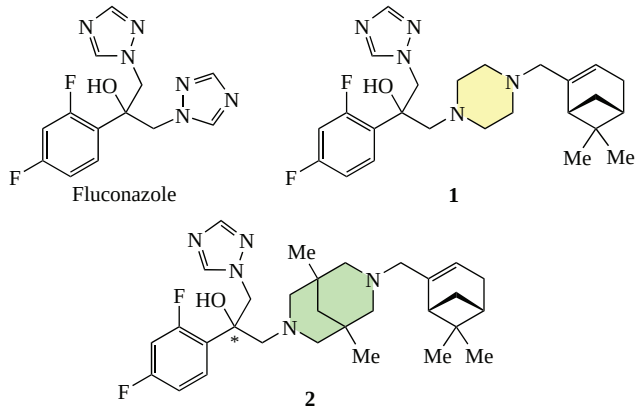

Figure 1 Fluconazole and monoterpene-containing azoles.

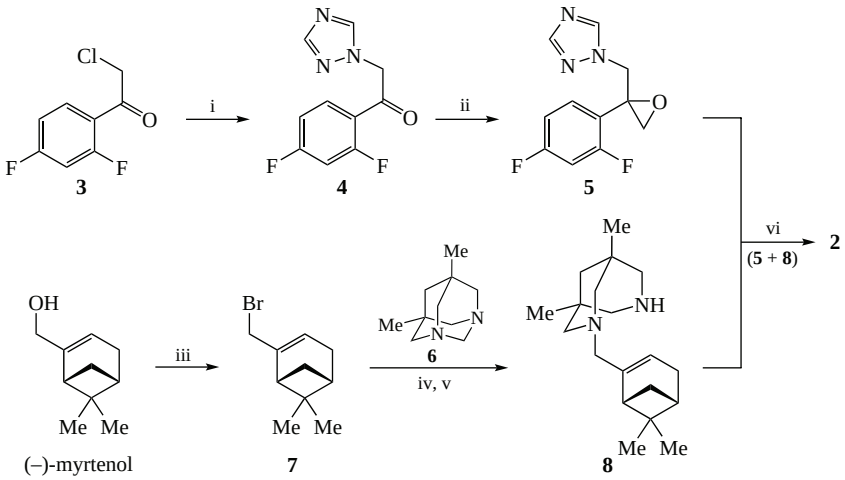

Scheme 1 *Reagents and conditions*: i, 1*H*-1,2,4-triazole, K_2CO_3, MeCN, reflux, 2 h, 80%; ii, $Me_3S^+OI^-$, NaOH (20% aq.), toluene, 60 °C, 4 h, 90%; iii, PBr_3, Et_2O, from −8 to 0 °C, 5 h, 95%; iv, 5,7-dimethyl-1,3-diazaadamantane **6**, benzene, reflux, 5 h; v, KOH, EtOH/H_2O, reflux, 4 h, 72%; vi, NEt_3, EtOH, reflux, 4 h, 55%.

(−)-myrtenyl bromide **7** with subsequent cleavage of quaternary ammonium salt (see Scheme 1).[11] The yield of product **8** over two steps was 72% (for details, see Online Supplementary Materials, Scheme S1). (−)-Myrtenyl bromide **7** was obtained by the reaction of (−)-myrtenol with PBr_3 as described.[12] Reaction of epoxide **5** with myrtenyl-bispidine **8** in the presence of NEt_3 was carried out by reflux in ethanol. After purification by column chromatography on SiO_2, product **2** was isolated with 55% overall yield. Compound **2** was formed as a mixture of two diastereomers, as confirmed by NMR spectroscopy data. Thus, the ^{19}F and ^{13}C NMR spectra contain two sets of signals of equal intensity with pairwise close chemical shifts. When analyzing the ^1H–^{13}C HSQC spectrum, it was determined that the ^1H NMR spectrum also consisted of two sets of signals of equal intensity. Analysis of the correlation spectra revealed the same sequence of arrangement of carbon atoms in both compounds, giving sets of signals. Exchange effects in the ^1H NMR spectra recorded at different temperatures (20–70 °C) were not observed, as well as exchange cross-peaks in 2D ^1H–^1H NOESY/EXSY, which excludes the possibility that the sets of signals belong to different conformations.

We evaluated the antifungal activity of **2** against a variety of *C. albicans* strains *in vitro* by determining their MIC values, which shows the minimum compound concentration to inhibit pathogen growth. Seven American Type Culture Collection (ATCC) fungal strains of *Candida* were included in the susceptibility tests performed using microdilution method (see Online Supplementary Material for details). Compound **2** demonstrated promising activity against one of the *C. albicans* strains (ATCC 64547). *C. albicans* (ATCC 90028) and *C. glabrata* were less susceptible to **2**, while *C. krusei*, an intrinsically azole-resistant fungus, was only susceptible to **2** at a high MIC similar to fluconazole. *C. parapsilosis* and *C. tropicalis* were completely resistant to **2** (Table 1). In general, the tested *Candida* strains were also less susceptible to **2** compared to **1** or fluconazole.

Azole antifungals act through inhibiting lanosterol 14α-demethylase (CYP51), a heme-dependent cytochrome P450 class enzyme that catalyzes the rate-limiting step of ergosterol biosynthesis in fungal membrane. Molecules of azole drugs are composed of three structural components: an azole ring providing axial coordination with the heme iron, an aromatic ring connected to the azole *via* an ethylene bridge, and a tail group attached to the ethylene linker, which occupies the active site gorge. Azoles such as fluconazole and oteseconazole have an additional

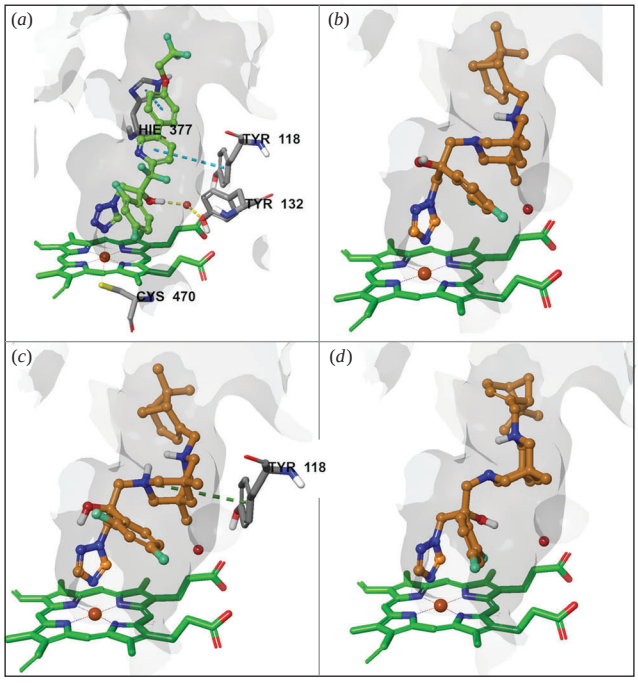

Figure 2 Co-crystallized binding of (*a*) oteseconazole[13] as well as predicted binding mode of forms of compound **2**: (*b*) *R*-**2**·H^+, (*c*) *R*-**2**·$2H^+$, and (*d*) *S*-**2**·H^+ in CaCYP51 active site. Ligands are represented as color ball-and-stick form (oteseconazole in yellow-green and forms of **2** in brown), amino acid residues as gray sticks, heme as green sticks, heme iron and water molecules as spheres, and electrostatic interactions as dashed lines. Protein active site molecular surface is rendered.

Table 1 MIC values (μg ml^{-1}) of compound **2** and close analogues against the selected *Candida spp*.

Sample	*Candida albicans* ATCC 64547	*Candida albicans* ATCC 90028	*Candida glabrata* ATCC 90030	*Candida krusei* ATCC 6258	*Candida parapsilosis* ATCC 22019	*Candida parapsilosis* ATCC 90018	*Candida tropicalis* ATCC 750
1[3]	0.03	0.016–0.03	0.5–2	0.5–1	0.06	0.008	0.016–0.03
2	4	8	8	16	>16	>16	>16
Fluconazole	0.25–0.5	<0.125	2–4	16–32	1–2	0.5–1	0.5–1

hydroxyl substituent on the ethylene linker that makes a critical water-mediated H-bond with a tyrosine residue of fungal CYP51s (*e.g.*, Tyr132 of *C. albicans* CYP51) [Figure 2(*a*)], which was reported to play a key role in CYP51 inhibitory potential of these azoles.[13–15]

Structure of **2** incorporates 1,2,4-triazole as azole ring, 2,4-difluorophenyl as aromatic group and a myrtenyl-bispidine as tail group, as well as a hydroxy substituent. Replacing the piperazine of **1** with a tricyclic isostere, bispidine, we expected better engagement with the active site gorge of fungal CYP51 and hence better activity than that of **1**, although the bioactivity data revealed otherwise. Due to the chirality of C^7 and the protonation potential of the nitrogens of bispidine, **2** was expected to occur as a mixture of two diastereomers with four protonation states for each making eight different entities. Spectral data confirmed the mixture of diastereomers, however molecular modeling predicted four entities, namely, *R*-**2**·H^+, *R*-**2**·$2H^+$, *S*-**2**·H^+ and *S*-**2**·$2H^+$ since only two protonated states (both bispidine nitrogens or only the nitrogen next to C^{21} are protonated) were calculated for each diastereomer under physiological conditions (pH 7 ± 2) (see Figure S9 in Online Supplementary Material for details). This finding suggests that, although **2** was obtained as a mixture of two diastereomers in deprotonated state through synthetic process, molecular modeling predicts that, under physiological conditions such as cell environment, each diastereomer of **2** should occur in two protonated states as indicated in Figure S9. Molecular docking of all four forms of **2** with *C. albicans* CYP51 (CaCYP51) predicted proper poses, as defined above for azoles, for only three their entities, *i.e.*, *R*-**2**·H^+, *R*-**2**·$2H^+$ and *S*-**2**·H^+. Docking scores suggested that the *R* enantiomer at C^7 showed higher affinity to CaCYP51 than its *S* enantiomer (Table S1). Docking poses for **2** showed a clear engagement with the heme ring *via* the triazole N^3 as axial ligand and electrostatic interaction with Tyr118, as well as van der Waals contacts with many key residues in the active site, especially by the myrtenyl moiety in the active gorge (Figure S10). However, the compound failed to make H-bond with Tyr132 unlike its piperazine analogue **1** [see Figure 2(*b*)–(*d*)].[3] Docking poses also revealed that the boat-like conformation of bispidine led to a bent-shape tail for **2** unlike **1** (Figure S11). The tail of **1** was predicted to assume a more upright orientation in our previous study.[3] The bent-shape tail of **2** predictably caused poor electrostatic engagement with the active site gorge and failure in water-mediated interaction with Tyr132, probably leading to more than 100-fold higher MICs for **2** compared to **1** against *C. albicans*.[3]

In summary, a new derivative with myrtenyl-bispidine fragment, 2-(2,4-difluorophenyl)-1-(7-{[(1*R*,5*S*)-6,6-dimethylbicyclo[3.1.1]hept-2-en-2-yl]methyl}-1,5-dimethyl-3,7-diazabicyclo[3.3.1]nonan-3-yl)-3-(1*H*-1,2,4-triazol-1-yl)propan-2-ol **2** was synthesized with a yield of 55%. The product was tested against various *Candida spp*. and found to exhibit activity against *C. albicans*. Molecular modeling predicted that **2** could act through fungal CYP51 inhibition. Molecular modeling also indicated conformational limitations of the bicyclic bispidine moiety leading to a less favorable fitting of **2** in CaCYP51 active site, which could be held accountable for **2**'s reduced efficacy compared to its piperazine analogue **1**.

The research was supported by the Russian Science Foundation (grant no. 22-73-00046). Biological and modeling studies were funded by Hacettepe University Scientific Research Projects Coordination Unit (Ankara, Turkey, grant no. TSA-2023-20443).The authors would like to acknowledge the Multi-Access Chemical Research Center SB RAS for spectral and analytical measurements.

Online Supplementary Materials

Supplementary data associated with this article can be found in the online version at doi: 10.1016/j.mencom.2024.01.036.

References

1 *Fungal Priority Pathogens List to Guide Research, Development and Public Health Action*, WHO, Geneva, Switzerland, 2022.
2 K. E. Pristov and M. A. Ghannoum, *Clin. Microbiol. Infect*., 2019, **25**, 792.
3 N. S. Li-Zhulanov, N. P. Zaikova, S. Sari, D. Gülmez, S. Sabuncuoğlu, K. Ozadali-Sari, S. Arikan-Akdagli, A. A. Nefedov, T. V. Rybalova, K. P. Volcho and N. F. Salakhutdinov, *Antibiotics*, 2023, **12**, 818.
4 L. E. Nikitina, S. A. Lisovskaya, V. A. Startseva, L. L. Frolova, A. V. Kutchin, O. G. Shevchenko, O. V. Ostolopovskaya, R. S. Pavelyev, M. A. Khelkhal, I. R. Gifanov, I. V. Fedyunina, R. R. Khaliullin, R. F. Akhverdiev, A. V. Gerasimov, E. V. Abzaldinova and A. G. Izmailov, *BioNanoScience*, 2021, **11**, 97.
5 A. Akhmedov, R. Gamirov, Yu. Panina, E. Sokolova, Yu. Leonteva, E. Tarasova, R. Potekhina, I. Fitsev, D. Shurpik and I. Stoikov, *Org. Biomol. Chem*., 2023, **21**, 4863.
6 A. V. Sofronov, I. S. Nizamov, L. A. Almetkina, L. E. Nikitina, D. G. Fatyhova, P. V. Zelenikhin, O. N. Il'inskaya and R. A. Cherkasov, *Russ. J. Gen. Chem*., 2010, **80**, 1267 (*Zh. Obshch. Khim.*, 2010, **80**, 1101).
7 I. S. Nizamov, L. A. Al'metkina, G. T. Gabdullina, R. R. Shamilov, A. V. Sofronov, L. E. Nikitina, S. A. Lisovskaya, N. I. Glushko and R. A. Cherkasov, *Russ. Chem. Bull*., 2012, **61**, 2370 (*Izv. Akad. Nauk, Ser. Khim.*, 2012, 2347).
8 N. O. Ilchenko, D. V. Sudarikov, R. V. Rumyantcev, D. R. Baidamshina, N. D. Zakarova, M. N. Yahia, A. R. Kayumov, A. V. Kutchin and S. A. Rubtsova, *Antibiotics*, 2022, **11**, 1548.
9 I. Tomassoli and D. Gündisch, *Curr. Top. Med. Chem.*, 2016, **16**, 1314.
10 M. I. Lavrov, P. N. Veremeeva, E. A. Golubeva, E. V. Radchenko, V. L. Zamoyski, V. V. Grigoriev and V. A. Palyulin, *Mendeleev Commun.*, 2022, **32**, 360.
11 E. V. Suslov, K. Y. Ponomarev, O. S. Patrusheva, S. O. Kuranov, A. A. Okhina, A. D. Rogachev, A. A. Munkuev, R. V. Ottenbacher, A. I. Dalinger, M. A. Kalinin, S. Z. Vatsadze, K. P. Volcho and N. F. Salakhutdinov, *Molecules*, 2021, **26**, 7539.
12 T. M. Khomenko, V. V. Zarubaev, I. R. Orshanskaya, R. A. Kadyrova, V. A. Sannikova, D. V. Korchagina, K. P. Volcho and N. F. Salakhutdinov, *Bioorg. Med. Chem. Lett*., 2017, **27**, 2920.
13 T. Y. Hargrove, L. Friggeri, Z. Wawrzak, A. Qi, W. J. Hoekstra, R. J. Schotzinger, J. D. York, F. P. Guengerich and G. I. Lepesheva, *J. Biol. Chem*., 2017, **292**, 6728.
14 M. V. Keniya, M. Sabherwal, R. K. Wilson, M. A. Woods, A. A. Sagatova, J. D. A. Tyndall and B. C. Monk, *Antimicrob. Agents Chemother*., 2018, **62**, e01134.
15 S. Sari, E. Koçak, D. Kart, Z. Özdemir, M. F. Acar, B. Sayoğlu, A. Karakurt and S. Dalkara, *Int. Microbiol*., 2021, **24**, 93.

Received: 18th July 2023; Com. 23/7214